RESEARCH ARTICLE

Sea surface salinity observed from the HY-2A satellite

Qingtao Song[1,2*] and Zhaohui Wang[1,2]

1. National Satellite Ocean Application Service, Beijing, 100081, China.
2. Key Laboratory of Space Ocean Remote Sensing and Application, State Oceanic Administration, Beijing, 100081, China.

Abstract: Motivated by the shortcomings of radio frequency interferences (RFI) associated with the spaceborne L-band radiometers near the Northwest Pacific and previous study near the Amazon plume, this study presents a sea surface salinity (SSS) retrieval algorithm from the microwave radiometer onboard the HY-2A satellite. The SSS signal is improved by differentiating the reflectance between the C and X band. A reflectance calibration method is proposed by using a combination of radiative transfer model (RTM) and the Klein-Swift emissivity model. Evaluations of the retrieved SSS from the HY-2A satellite indicate that the root mean square error (RMSE) is about 0.35 psu on 0.5 degree grid spacing and monthly time scale which is comparable to the accuracy of SMOS and Aquarius-SAC/D satellites.

Keywords: Sea surface salinity, microwave radiometer, HY-2A satellite, SMOS, Aquarius, emissivity model

*Correspondence to: Qingtao Song, National Satellite Ocean Application Service, Beijing, China, 100081, Beijing, China. Email: qsong@mail.nsoas.org.cn.

1. Introduction

Sea surface salinity (SSS), the saline concentration of near-surface sea water, partially determines the dielectric constant of water which in turn determines the emissivity of sea water into the atmosphere. With the advent of space-borne microwave radiometers that directly measure the brightness temperatures (T_B) at th e top of the atmosphere, the relationship between T_B and SSS can be thus theoretically established through atmospheric radiation transfer physics model and emissivity or reflectance model near the sea surface (Klein and Swift, 1977).

The relationship between brightness temperature and sea surface salinity is discernable at the lower range of microwave bands (approximately from 1.0 GHz to 10.0 GHz) in which sea surface emissivity varies with varying salinity. The T_B-SSS relationship is especially pronounced around 1.4 GHz (L-band) and both current spaceborne salinity missions are therefore operated at L-band.

The current satellite missions that measure sea surface salinity include the Soil Moisture and Ocean Salinity (SMOS) satellite (Yin, Boutin, Dinnat *et al.*, 2016) and the Aquarius/Satélite de Aplicaciones Científicas (Aquarius/SAC-D) satellite (Lagerloef *et al*, 2008). The SMOS mission, launched in November 2009, is operated by the European Space Agency (ESA), and the Aquarius/SAC-D mission was launched in June 2011 jointly operated by the National Aeronautics and Space Administration (NASA) o f the United States and the Argentina Comisión Nacional de Actividades Espaciales (CONAE). Both SMOS and Aquarius/SAC-D provide global SSS observations from 10-day to monthly interval.

Though numerous studies have demonstrated applications of the SMOS and Aquarius/SAC-D observations in oceanography and marine meteorology, the accuracy in terms of root mean square error (RMSE) compared with in s itu observations from the two missions varies from 0.3 psu to 0.5 psu averaged over a 100 km × 100 km domain on a monthly time scale (Reul *et al*, 2012). The error sources for the

L-band radiometer on orbit are primarily from cosmic background radiation, atmospheric ionic interference, surface emissivity model, and most importantly from the system design. For example, the payload of the SMOS, the Microwave Imaging Radiometer by Aperture Synthesis (MIRAS), is a Y-shape two-dimensional (2D) aperture synthesis radiometer with 69 antennas. The topography of the 69 antennas and imaging geometry require tremendous efforts in inter-calibration of the individual sensors in the Y-shape frame.

Moreover, the SMOS observations severely suffered from the radio frequency interferences (RFIs) around 1.4 GHz. Regions of the RFIs around 1.4 GHz include parts of Europe, East Asia, Southern Asia, and the Middle East. The quality of the SMOS data near the Northwest Pacific is significantly contaminated and operationally flagged as invalid observations. While future regulations of the ground radar stations operating around L-band are required to avoid the L-band contamination of the spaceborne sensors, the losses of the SSS observations have thus limited applications of the SMOS data in the Northwest Pacific.

Of particular interest to this study, the SSS information can also be retrieved from microwave bands higher than 1.4 GHz, which is free from the major L-band RFIs near the coast of the Pacific. It has been demonstrated that the SSS can be retrieved by combining 6 (C band) and 10 GHz (X band) brightness temperature from the Advanced Microwave Scanning Radiometer on the Earth Observing System Aqua satellite (AMSR-E). Reul *et al*. (2009) reported that the retrieved SSS on 0.5 degrees grid in a bimonthly scale over the region of the Amazon plume show relative accuracy similar to that of the SMOS observations.

Similar to the system design of AMSR-E, the radiometer onboard the HY-2A satellite has acquired a large amount dataset since its launch in 2011. The HY-2A satellite is the first microwave satellite in China that is specifically designed to measure global observations of sea surface temperature, sea surface winds, and sea surface height with multiple sensors onboard (Huang *et al*, 2014).

Motivated by the shortcomings of the RFI associated with the L-band near the Northwest Pacific and independent evidence from the study of Reul *et al*. (2012), the purposes of this study are 1) to analyze the emissivity properties of the C and X band near the sea surface, 2) to calibrate the T_B at C and X band of HY-2A satellite, and 3) to retrieve the sea surface salinity on the monthly scale by differentiating the emissivity at C and X band of the HY-2A satellite.

2. The HY-2A Satellite

The HY-2A satellite is designed to globally measure the ocean dynamic environment parameters (sea surface height, significant wave height, sea surface winds and sea surface temperature). Launched on August 16 2011, the HY-2A satellite is the third ocean satellite of China following the HY-1A and HY-1B satellites, and the first ocean dynamic environment satellite. HY-2A carries active and passive microwave sensors, and high accuracy orbit tracking and determination system, with all-weather, 24-h, and global measuring capability. The HY-2A scanning microwave radiometer is consisted of nine microwave bands from 6.6 GHz to 37 GHz (Table 1).

Table 1. Specifications of the HY-2A scanning radiometer.

Frequency (GHz)	6.6	10.7	18.7	23.8	37.0
Polarization	VH	VH	VH	V	VH
Swath	>1600 km				
Footprint (km)	100	70	40	35	25
Precision (k)	< 0.5				<0.8
Calibration precision (K)	1.0（180～320）				
Dynamic range (K)	3～350				

The objective of the HY-2A microwave radiometer is to acquire global observations of the sea surface temperature, wind speed, and cloud liquid water. The nine microwave bands range from 6.6 GHz to 37 GHz with both vertical and horizontal polarizations (except V-pol only for 23.8 GHz). As shown in Figure 1, the response of the sea surface reflectance to sea surface salinity is sensitive near 1.4 GHz and drops sharply as microwave frequency increases for a given SST for both horizontal and vertical polarizations (H-pol and V-pol), while the signal is stronger for the V-pol.
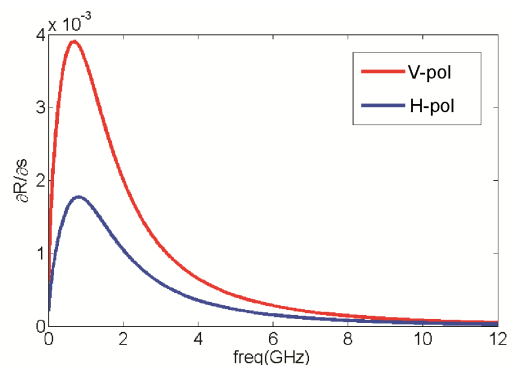

Figure 1. Response of sea surface reflectance to sea surface salinity as a function of frequency computed from Klein and Swift (1977) for the salinity of 35 psu and temperature of 300 K with a fixed incident angle.

The focus of this study is on the C and X bands in which the response of sea surface radiation to changing SSS is apparently less sensitive than that in the L band. However, the characteristics of the response of reflectance to SSS and SST are different between the C and X band. To demonstrate the capability of C/X band measuring the sea surface salinity, the reflectance of the sea surface in microwave bands is computed as functions of SSS and SST (Figure 2) following Klein and Swift (1977, see also Appendix). For a given SST, the surface reflectance increases monotonically with increasing SSS, while the emissivity of sea surface decreases due to the presence of saline materials that increase the dielectric properties of sea water and thus decrease the emissivity. Given the fact that sea water is opaque to microwaves, the sum of emissivity and reflectance at the sea surface is constant. Meanwhile, for a given SSS, the surface emissivity (reflectance) increases (decreases) due to higher molecular energy with higher temperature (Figures 2A and 2B). By differentiating the reflectance between the C and X band, it is clearly seen in Figure 2C that both SSS and SST have apparent impacts on the differential reflectance of sea surface, which is defined as:

$$\Delta R_{KS} = R_{10.7V} - R_{6.6V}, \qquad (1)$$

where $R_{10.7V}$ and $R_{6.6V}$ are computed at 10.7 GHz and 6.6 GHz band, respectively, in V-pol using the Klein and Swift (KS) model. The brightness temperature T_B at the top of the atmosphere contains information for both SSS and SST.

3. Methodology

From a complete data processing perspective, the SSS retrieval procedure from the HY-2A satellite includes data preprocessing from raw data (Level 0) of the scanning radiometer of HY-2A satellite to brightness temperature T_B, data regrouping of the T_B for the nine microwave channels and applying geophysical retrieval algorithm (multiple linear regression) to obtain the Level 2 products (SST, surface wind speed, cloud liquid water, and columnar water vapor). The data processing is managed and operated at the ground application segment of the National Satellite Ocean Application Service (Huang, Zhu, Lin *et al*., 2014). Meanwhile for the SSS retrieval as discussed in Section 2, besides the two channels (C and X band) in vertical polarization used in this study, the World Ocean Atlas 09 (WOA09) salinity climatology from the National Oceanic and Atmospheric Administration (NOAA) was also used to calibrate the HY-2A T_B.

As listed in Table 1 in Section 2, the antenna of the HY-2A radiometer maintains a constant forward viewing incident angle of 47.7°. The instrument is capable of providing a swath of 1,600 km on the Earth surface for each rotation.

In passive microwave ocean remote sensing, the radiative transfer model (RTM) determines the brightness temperature at the top of the atmosphere from the ocean surface radiation passing through the atmosphere. The typical expression of T_B is as follows:

$$T_B = T_{BU} + \tau[ET_s + T_{B\Omega}], \qquad (2)$$

where T_B is the brightness temperature of the radiometer, T_{BU} is the upwelling atmospheric brightness temperature, $T_{B\Omega}$ is the sky radiation scattered upward by the Earth surface, T_s is the SST, τ is the atmospheric transmissivity which is affected primarily by the atmospheric temperature and humidity profiles, and E is the sea-surface emissivity. $T_{B\Omega}$ can be generally expressed as:

$$T_{B\Omega} = R \cdot M, \qquad (3)$$

where R is sea surface reflectance. Assuming the microwave energy is in equilibrium and sea surface is
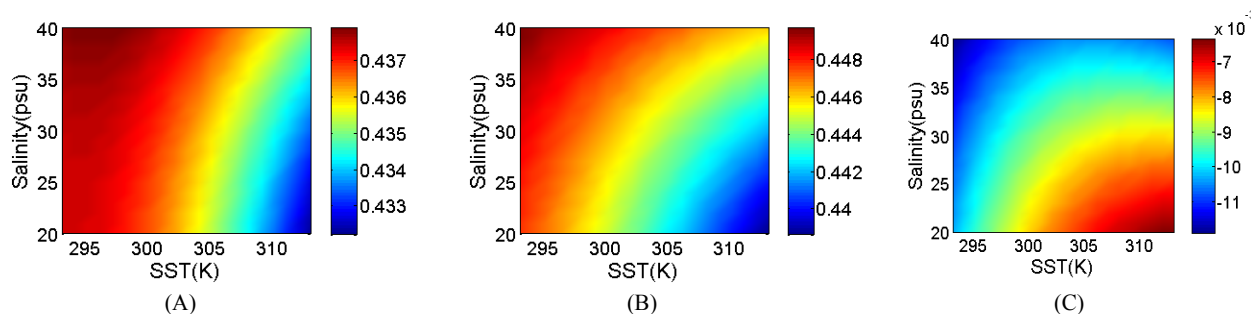

Figure 2. Reflectance of sea surface in microwave bands as functions of SSS and SST. (A) Reflectance at 10.7 GHz (X band) in V-pol of the HY-2A radiometer, (B) reflectance at 6.6 GHz (C band) in V-pol of the HY-2A radiometer, and (C) reflectance difference between the 10.7 GHz and 6.6 GHz.

opaque to the microwave band, $R=1-E$ according to the Kirchhoff thermal radiation law. In Equation (3) M is a function of the downwelling atmospheric radiation, atmospheric transmissivity, corrections to the sea surface scattering, and cosmological background radiation.

The sea surface reflectance R can be derived from Equations (2) and (3):

$$R = \frac{(T_B - T_{BU}) / \tau - T_s}{M - T_s}, \qquad (4)$$

Since all the variables in Equation (4) can be computed from a radiative transfer model, the sea surface reflectance R is thus related to the brightness temperature T_B of the satellite radiometer. As described in Appendix and Equation (1), R is also related to the sea surface salinity through the ocean surface emissivity model. The KS emissivity model used in this study is an empirical model that relates the R to SSS and SST. By combining the RTM and the KS model, sea surface salinity can be retrieved from T_B, where R is a key parameter that bridges SSS and T_B.

First, the T_B of the HY-2A radiometer is converted to the reflectance R by using the RTM at C (6.6 GHz) and X (10.7 GHz) bands, and thus the observed differential reflectance ΔR_{HY-2A} can be obtained from the HY-2A radiometer

By using the radiometer SST product and SSS from the WOA09, the modeled reflectance ΔR_{KS} is computed with the KS model at C and X band. The

ΔR_{HY-2A} observed by the HY-2A satellite is calibrated with the modeled ΔR_{KS} for the next step of SSS retrieval (Figure 3).
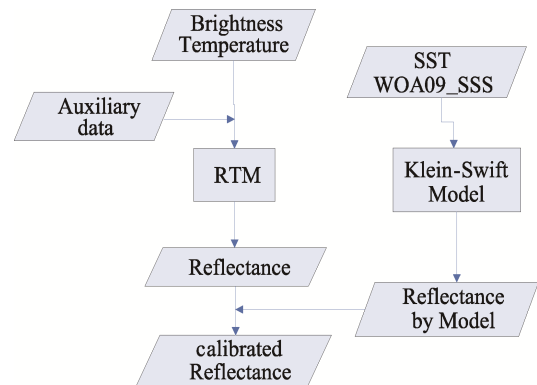

Figure 3. Reflectance calibration procedure for the HY-2A radiometer. Brightness temperature is from the HY-2A radiometer, and the auxiliary data include SST, wind speed, cloud liquid water, and water vapor used in the RTM. In KS model, SST from the radiometer and SSS from the WOA09 were used.

The calibration procedure consists of two steps. Firstly, the matchups for ΔR_{HY-2A} and ΔR_{KS} were selected and the calibration coefficients for ΔR_{HY-2A} were computed through the least-square fit for each month (Figure 4). The calibration coefficients for each month are statistically stable and do not change much with time. Secondly, the SSS products were then retrieved by using the calibrated ΔR_{HY-2A} between C and X bands of the HY-2A radiometer.
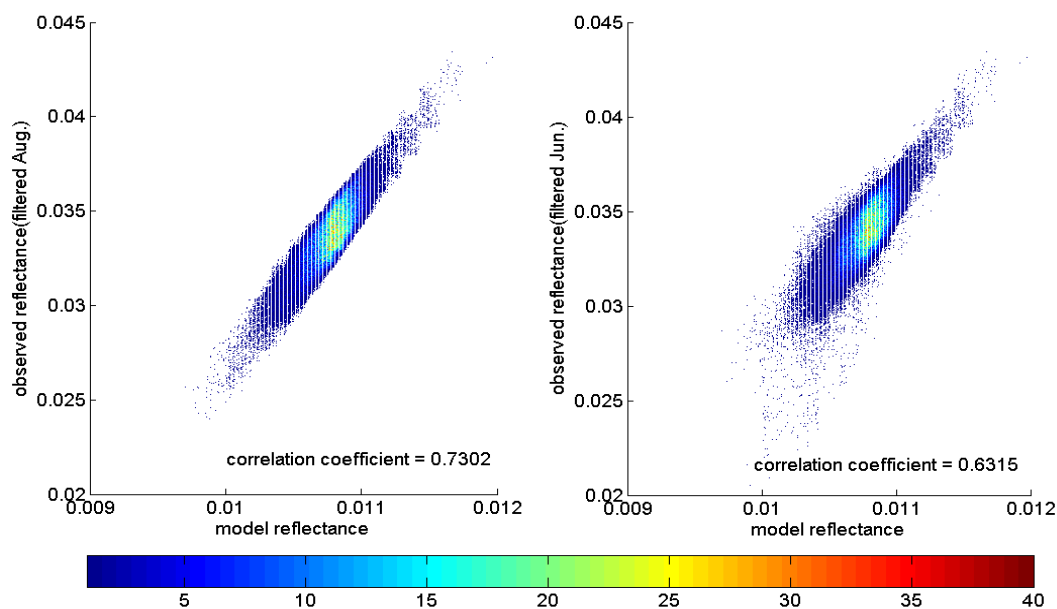

Figure 4. Calibrated reflectance versus and KS model reflectance of HY-2A for the months of (left) August 2012 and (right) June 2012

4. Results

Once the differentiated reflectance data for the HY-2A are constructed, it is straightforward to obtain HY-2A SSS product by finding solutions from the SSS-ΔR_{HY-2A} lookup table (Figure 5). The retrieved SSS is gridded with 0.5 degree latitude by 0.5 degree longitude on a monthly scale. Map of the sea surface salinity retrieved from the HY-2A radiometer for August 2012 is shown in Figure 6. In comparisons with the WOA09 climatology, the HY-2A-retrieved SSS presents reasonable features of the freshwater runoff near the Yangtze Delta. For the SSS retrievals in the Northwest Pacific, the results show mesoscale features of the SSS in the South China Sea. Following the same SSS retrieval algorithm for the HY-2A satellite, one-year data of the SSS retrievals from July 2012 to June 2013 were processed (Figure 7) over the Northwest Pacific and further evaluated by comparing with the WOA09 SSS for each month. For the one-year data presented in this study, the root means square error (RMSE) of the HY-2A SSS is about 0.56 psu on a monthly time scale for the SSS product of the HY-2A swath (along with the track, Figure 8A). The

RMSE is significantly reduced to 0.35 psu after the SSS swath data are bilinearly interpolated to the 0.5 degrees by 0.5 degrees grid spacing (Figure 8B), which is comparable to the accuracy of SMOS and Aquarius/SAC-D.
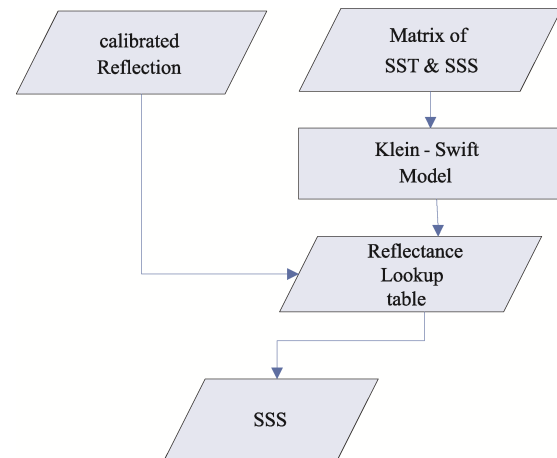

Figure 5. SSS retrieval procedure for the HY-2A radiometer. The reflectance lookup table is computed from the KS model by using radiometer SST data and SSS (WOA09) data. The final SSS is retrieved from HY-2A radiometer by selecting the best approximation in the lookup table.
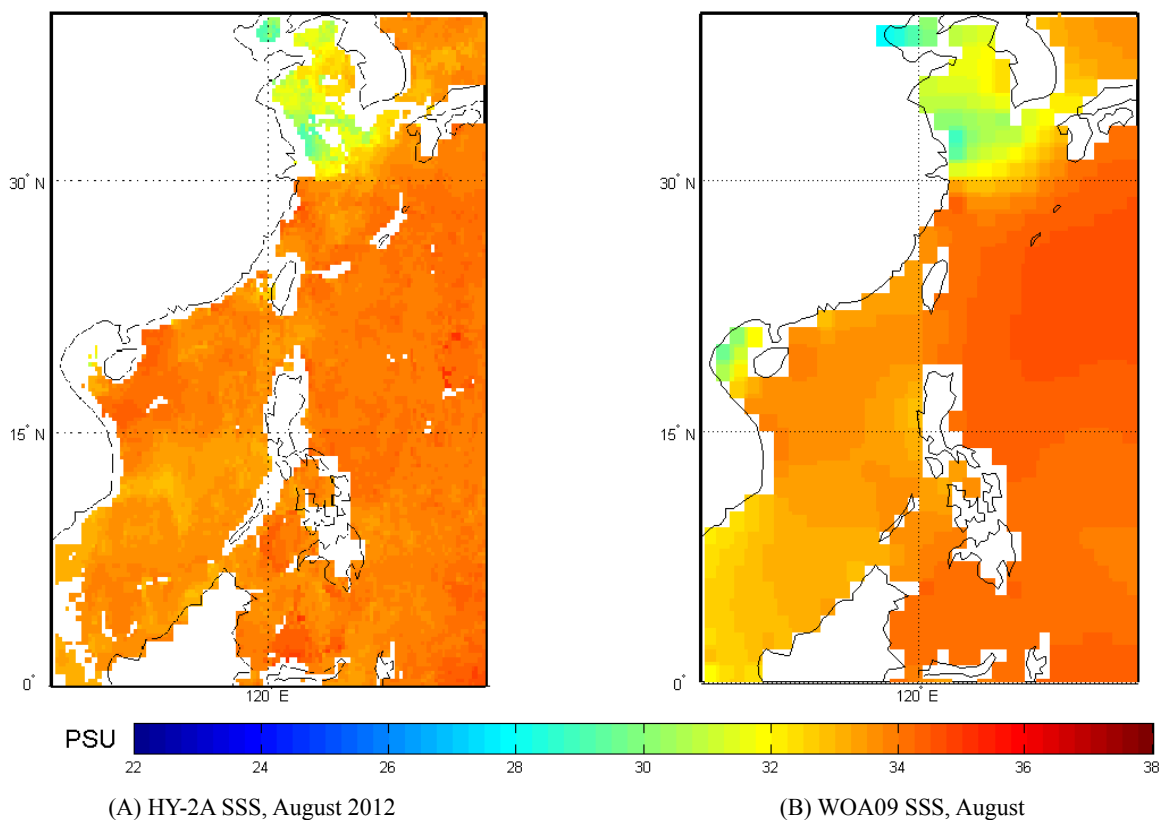

(A) HY-2A SSS, August 2012   (B) WOA09 SSS, August

Figure 6. Map of SSS retrieved from the HY-2A radiometer for (A)August 2012 versus (B) WOA09 SSS.
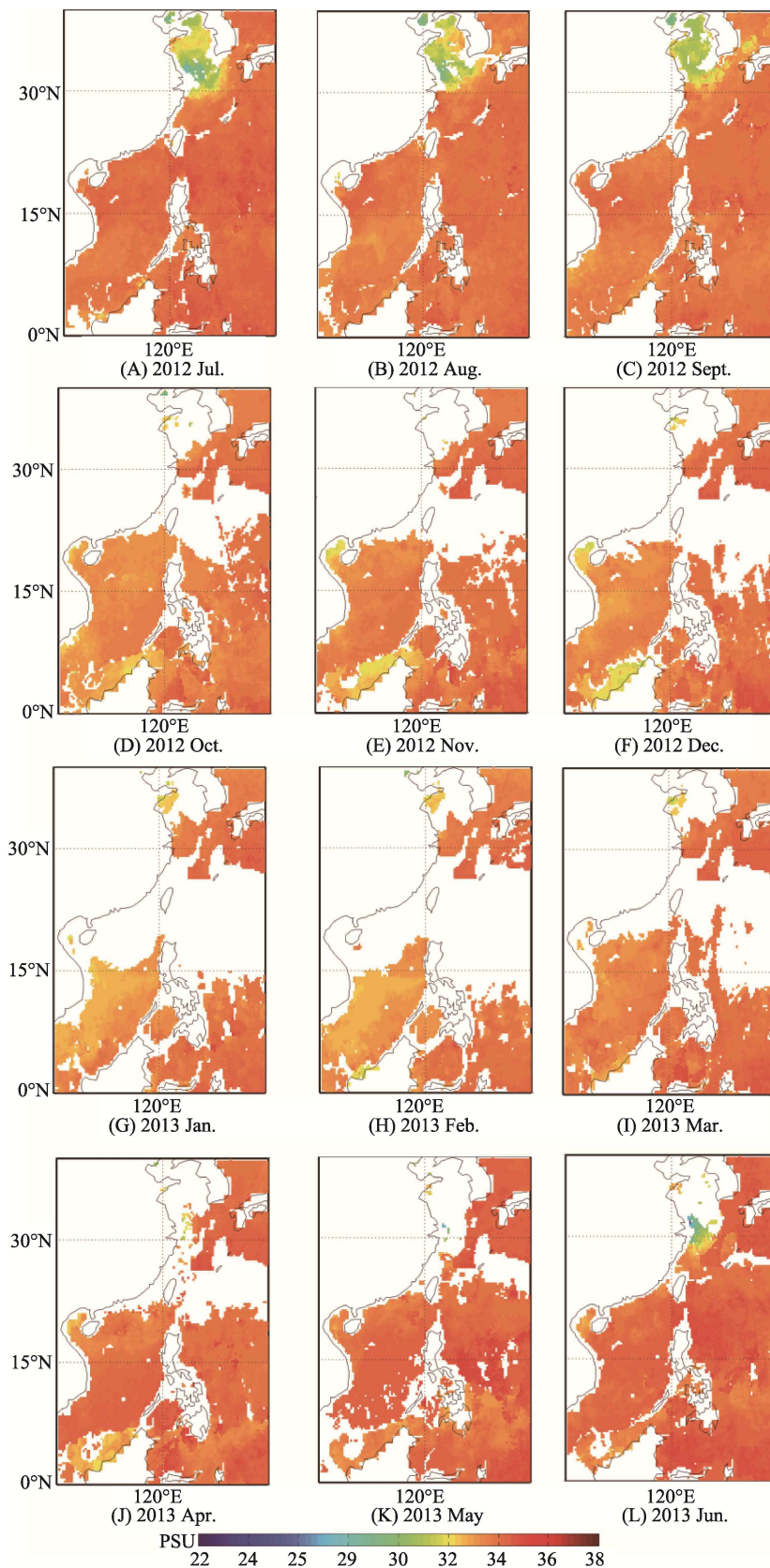
Figure 7. Maps of the SSS retrieved from the HY-2A satellite from July 2012 to June 2013. Low-quality SSS data were rejected (white region for each panel).
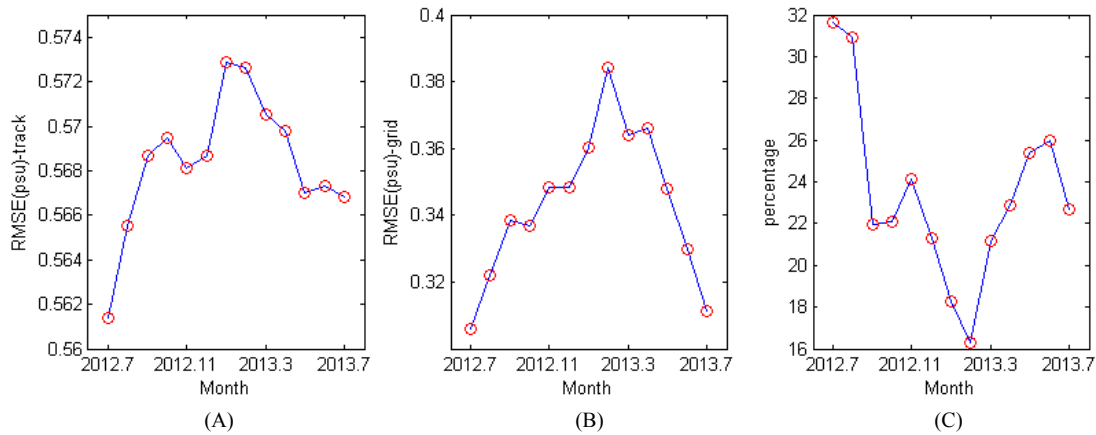
Figure 8. Evaluation of the SSS retrieved from the HY-2A satellite from July 2012 to June 2013. (A) Root mean square error (RMSE) of SSS compared with WOA09 SSS along the satellite track, (B) RMSE of the grid SSS product, and (C) percentage of the valid data retrieved from the HY-2A satellite.

5. Discussion

This study presented an algorithm of the sea surface salinity retrieval from the microwave radiometer onboard the HY-2A satellite. Though the response of sea surface reflectance to surface salinity is relatively weak in the C and X band compared with L-band used on the SMOS and Aquarius-SAC/D satellite missions, the SSS signal is significantly improved after differentiating the sea surface reflectance between the C and X band. A reflectance calibration method is proposed in this study by using both the radiative transfer model (RTM) and Klein-Swift emissivity model. SSS of the HY-2A satellite is then retrieved by finding the best solution in the lookup table constructed from the Klein-Swift model using the radiometer-derived sea surface temperature (SST) and WOA09 SSS data.

Evaluations of the retrieved SSS from the HY-2A satellite indicate that the RMSE is about 0.35 psu on a 0.5-degree grid spacing on a monthly time scale, which is comparable to the accuracy of SMOS and Aquarius-SAC/D satellites. The SSS dataset from the HY-2A satellite are free of the RFI contaminations in the Northwest Pacific, thus providing valuable sea surface salinity observations for studies in the northwest Pacific.

It should be noted that five ocean satellites equipped with radiometers are scheduled to be launched within the next five to ten years in China. The SSS retrieval method proposed in this study for the HY-2A satellite is also applicable to similar radiometers with C and X bands of the follow-on satellite missions. With a refined radiative transfer model and emissivity model, the accuracy of SSS retrieved from the C/X band is expected to be improved.

Conflict of Interest

No conflict of interest was reported by all authors.

Acknowledgments and Funding

Appendix

The Klein-Swift emissivity model

The emissivity of the flat sea surface in the thermal equilibrium state is directly related to the surface reflectance through $E=1-R$, where R is the Fresnel amplitude reflection coefficient.

$$Ri(\theta) = \left| \rho i(\theta) \right|^2$$

$$\rho_v = \frac{n^2 \cos\theta - \sqrt{n^2 - \sin^2\theta}}{n^2 \cos\theta + \sqrt{n^2 - \sin^2\theta}}$$

$$\rho_h = \frac{\cos\theta - \sqrt{n^2 - \sin^2\theta}}{\cos\theta + \sqrt{n^2 - \sin^2\theta}}$$

$$n \cong \sqrt{\varepsilon}$$

where θ is incident angle, R is reflectance, v is vertical polarization, h is horizontal polarization, n is complex refractive index, and ε is a complex

dielectric constant.

The complex dielectric constant of sea water may be calculated at any frequency within the microwave band from the Debye expression that in its most general form, is given by:

$$\varepsilon = \varepsilon_\infty + \frac{\varepsilon_S - \varepsilon_\infty}{1 + (j\omega\tau)^{1-\alpha}} - j\frac{\sigma}{\omega\varepsilon_0}$$

where $\omega = 2\pi f$ is the radian frequency with f in Hertz, ε_∞ is the dielectric constant at infinite frequency, ε_S is the static dielectric constant, τ is the relaxation time in seconds, σ is the ionic conductivity in mhos/meter, α is an empirical parameter that describes the distribution of relaxation times, and $\varepsilon_0 = 8.854 \times 10^{-12}$ is the permittivity of free space in farads/meter.

$\varepsilon_\infty = 4.9$ and $\alpha = 0$ were assigned as constant values, respectively. ε_S, τ, and σ are functions of the temperature and salinity of seawater and experimentally determined. The regression equation for the ionic conductivity of sea water, as derived by Weyl (1964) and modified by Stogryn (1971), is defined by the following relationships:

$$\sigma(T, S) = \sigma(25, S)\exp(-\Delta\beta)$$
$$\Delta = 25 - T$$
$$\beta = 2.033 \times 10^{-2} + 1.266 \times 10^{-4}\Delta +$$
$$2.464 \times 10^{-6}\Delta^2 - S(1.849 \times 10^{-5} -$$
$$2.551 \times 10^{-7}\Delta + 2.551 \times 10^{-8}\Delta^2)$$
$$\sigma(25, S) = S(0.182521 - 1.46192 \times$$
$$10^{-3}S + 2.09324 \times 10^{-5}S^2 -$$
$$1.28205 \times 10^{-7}S^3)$$

where T is the temperature in degrees Celsius and S is the salinity in parts per thousand.

ε_S is given by Ho and Hall (1973):

$$\varepsilon_S(T, S) = \varepsilon_S(T)a(S, T)$$
$$\varepsilon_S(T) = 87.134 - 1.949 \times 10^{-1}T -$$
$$1.276 \times 10^{-2}T^2 + 2.491 \times 10^{-4}T^3$$
$$a(S, T) = 1.000 + 1.613 \times 10^{-5}ST - 3.656 \times$$
$$10^{-3}S + 3.210 \times 10^{-5}S^2 - 4.232 \times 10^{-7}S^3$$

The expression for the relaxation time, τ, is

retained for the modeling of the dielectric constant and is given by Stogryn (1971):

$$\tau(T, S) = \tau(T, 0)\,b(S, T)$$
$$\tau(T, 0) = 1.768 \times 10^{-11} - 6.086 \times 10^{-13}T +$$
$$1.104 \times 10^{-14}T^2 - 8.111 \times 10^{-17}T^3$$
$$b(S, T) = 1.000 + 2.282 \times 10^{-5}ST - 7.638 \times$$
$$10^{-4}S - 7.760 \times 10^{-6}S^2 + 1.105 \times 10^{-8}S^3$$

Reference

Huang X, Zhu J, Lin *et al*. (2014). Preliminary Assessment of Sea Surface Wind Speed Production of HY-2 Scanning Microwave Radiometer. *Acta Oceanologica Sinica*, 33(1): 114–119.
http://dx.doi.org/10.1007/s13131-014-0403-z.

Klein L and Swift C T. (1977). An improved model for the dielectric constant of sea water at microwave frequencies. *Antennas and Propagation, IEEE Transactions on,* 25(1): 104–111.
http://dx.doi.org/10.1109/TAP.1977.1141539.

Lagerloef G, Colomb F R, Vine D L *et al*. (2008). The Aquarius/Sac-D Mission: Designed to Meet the Salinity Remote-Sensing Challenge. *Oceanography*, 21(1): 68–81.
http://dx.doi.org/10.1109/TAP.1977.1141539.

Reul N, Tenerelli J, Boutin J *et al*. (2012). Overview of the First SMOS Sea Surface Salinity Products. Part I: Quality Assessment for the Second Half of 2010. *IEEE Transactions on Geoscience and Remote Sensing*, 50(5): 1636–1647.
http://dx.doi.org/10.1109/TGRS.2012.2188408.

Reul N, Saux-Picart S, Chapron B *et al*. (2009), Demonstration of ocean surface salinity microwave measurements from space using AMSR-E data over the Amazon plume. *Geophysical Research Letters*, 36(13): 88–97
http://dx.doi.org/10.1029/2009GL038860.

Stogryn A. (1971). Equations for Calculating the Dielectric Constant of Saline Water (Correspondence). *IEEE Transactions on Microwave Theory & Techniques*, 19(8): 733–736.
http://dx.doi.org/10.1109/TMTT.1971.1127617.

Weyl P K (1964). On the Change in Electrical Conductance of Seawater with Temperature. *Limnology & Oceanography*, 9(1): 75–78.
http://dx.doi.org/10.4319/lo.1964.9.1.0075.

Yin X B, Boutin J, Dinnat E *et al*. (2016). Roughness and foam signature on S MOS-MIRAS brightness temperatures: a semi-theoretical approach. *Remote Sensing of Environment*, 180: 221–233.
http://dx.doi.org/10.1016/j.rse.2016.02.005.